Int J Adv Manuf Technol (2016) 82:1693–1705
DOI 10.1007/s00170-015-7491-6

ORIGINAL ARTICLE

Experiment-based thermal error modeling method for dual ball screw feed system of precision machine tool

Hu Shi[1,2] · **Dongsheng Zhang**[1] · **Jun Yang**[1] · **Chi Ma**[1] · **Xuesong Mei**[1] · **Guofang Gong**[2]

Received: 30 January 2015 / Accepted: 22 June 2015 / Published online: 11 July 2015

Abstract In order to investigate the thermal behavior of a dual ball screw feed drive system of a precision boring machine tool, experimental study on and theoretical modeling of thermally induced error along with heat generation characteristics are conducted in this paper. Experiments are carried out on the machine tool to measure and collect the thermodynamic information with its feed drive system operating under different working conditions. Based on the real-time data of the thermal expansion of ball screw in the axial direction, relationships between the thermal error and axial elongation are established to predict the thermal error distribution. The results show that the thermal error varies with different working position through the ball screw length linearly and with working time nonlinearly. In addition, another simplified way to model thermal error is presented to overcome the difficulties existing in the ball screw feed drive system of which the axial elongation is hard to collect. Fuzzy clustering and linear regression methods are employed to carry out the theoretical modeling of thermal error and optimization to sift out the critical heat sources. With the temperature data of these critical heat generation points, the thermally induced error of the ball screw feed drive system can be predicted easily alternatively. Experiments under a different condition are preformed to verify both prediction and modeling methods. It turns out that the proposed prediction methods are effective and practical to be used in the machining process as well.

✉ Hu Shi
shihufw@163.com

[1] School of Mechanical Engineering, Xi'an Jiaotong University, Xi'an 710049, China

[2] State Key Laboratory of Fluid Power Transmission and Control, Zhejiang University, Hangzhou 310027, China

Keywords Thermal error modeling · Error prediction · Feed system · Fuzzy cluster · Linear regressions

1 Introduction

Heat generation in machine tools has a considerable influence on both mechanical structure deformation, and thermally induced error consequently reduces the geometrical and machining accuracy. It is proven in the previous research that thermal errors account for up to 75 % of the total errors of machined work pieces when it comes to precision machining [1]. Therefore, special attentions are paid on his topic in the recent research activities.

Many factors contribute to the thermal error of a machine tool, such as thermal deformation of spindle specified in many studies [2]. The thermal error that arises in ball screw system to be discussed in this paper plays a great important role. In the past decades, great efforts have been taken to minimize the thermal effects on the machining accuracy especially for precision CNC machine tools, including error measurement, modeling, prediction, and heat generation reduction. In addition, to separate the total errors of machine tool, methods for uncertainty budget calculation and the classification of errors in machine tools were properly proposed [3, 4].

In order to investigate the thermal effect, theoretical modeling, predicting, and optimization analysis based on numerical simulation are frequently performed [5–7]. Kim et al. estimated the two-dimensional temperature distributions of a ball screw system at various moving speeds by finite element method [8]. Ming et al. developed an integrated thermal model using the finite element method to analyze the temperature distribution of a ball screw feed drive system, considering the thermal contact resistance

between the bearing and its housing [9]. Ahn et al. formulated the heat transfer problems of the ball screw system and designed an observer to estimate the whole temperature field [10]. Otakar carried out a closed loop finite element analysis and developed numerical models to confirm the influence of bearing preload on thermal stability of the ball screw drive system [11]. Temperature rise of the ball screw system directly leads to deformation of the metallic components, and thermal expansion caused by heat generation adversely reduces the machining accuracy. Wu et al. analyzed the relationship between temperature increase and thermal deformation of a ball screw feed drive system and estimated the strength of the heat source with the measured temperature profile by inverse analysis [12]. Huang selected front bearing and nut and back bearing as independent variables and used multiple regression method to analyze the thermal deformation of a ball screw feed drive system [13] and failed to consider the ambient temperature. Yun et al. used finite element method to estimate the thermal behavior of the ball screw and guide way with experimental verification [14].

Error compensation is the final objective of thermal-related research, and various compensation methods are proposed by researchers. Wu et al. developed a new technique to reduce the error by detecting the thermal expansion and sending a feedback to the microprocessor after calculation with the mathematical models built in advance [15]. Wang et al. presented a new approach for real-time compensation of geometric and thermal errors based on Newton interpolation method [16]. Hsieh et al. proposed a control scheme for a mechanically coupled dual ball screw system to decrease the positioning error that appears under the actual working conditions [17].

On the other hand, researchers have been taking great efforts on balancing the heat generated in the feed drive systems. Mayr et al. proposed different cooling concepts for ball screw systems and made comparisons by simulation study [18]. Xu et al. designed an air cooling ball screw system to avoid thermal errors. In this way, the feed drive system can achieve thermal equilibrium faster and reduce the peak temperature rise effectively [19, 20]. Yang et al. applied the computational approach to estimate the influence of different cooling conditions on thermal deformation and indicated that the positioning accuracy can be improved through some effective cooling measures [21]. Liu et al. developed a cooling device and embedded it in the ball screw drive system to cool the high-speed units [22].

It can be seen that numerical computation-based simulation accompanied by measurement is a very effective way to address the thermal issues concerned in feed drive systems. However, it is difficult to build an accurate mathematical model considering the uncertainties in heat transfer. Cooling is of great significance to counterbalance the heat generated by components, but it is complicated to some extent and costly to incorporate an additional cooling system. Therefore, error prediction helps definitely to perform compensation and improve the positing accuracy of feed drive systems.

In this paper, simple but practical modeling methods for thermal errors are proposed with approximation of error variation with time and position as well as optimization of heat source. They are easy to implement and turn out to have a relatively predicting accuracy, really suitable for applications as online monitoring and compensation. Different from the previous research, we take a complete precision boring machine tool in the workshop into account, providing a more convicting working condition with real operation. This paper firstly measures and models the thermal characteristics. Then, the simplified thermal error predicting models of the ball screw feed drive system are presented based on mathematical and experimental analysis, in the presence of real-time detecting certain critical variables. Finally, models and the predicting method are verified by experiments under different working conditions.

2 Experimental setup

Figure 1 shows a box-in-box structurized precision boring machine tool located in a constant-temperature workshop. It has three moving axes with dual ball screw drive on each axis. The maximum feed speed along each axis of the machine tool is 40 m/min, and the corresponding stroke of the worktable is 1200 mm. The worktable reciprocates in the section with a length of 1100 mm. Heat of the ball screw system is mainly generated by friction between moving nut and ball screw, as well as the rotating bearings at both ends. To investigate the thermal characteristics of the ball screw system in the *x*-axis, both temperature rise and thermal expansion are measured in this study. Besides, screw shafts to be tested are preloaded by an amount of 47 μm.

To obtain the thermal behavior of the ball screw system, nine heating points are measured corresponding to one ball screw system, as shown in Fig. 2. For each ball screw, three thermocouples are located on the surface of electric motor and front and rear bearing supports, respectively. One thermocouple is fixed on the surface of each moving nut. The last one is used to measure the room temperature. Besides, temperature of the ball screw surface is measured by infrared imaging because the thermocouples cannot be attached on the ball screw surface in contact with the moving nut.

Thermal errors are measured in two ways. An eddy current displacement sensor is mounted against the rear side of the ball screw in the direction perpendicular to the side surface as shown in Fig. 3, also shown as S1 in Fig. 2. It is assumed that the ball screw is fixed at one end; this probe can record the overall thermal expansion of the ball screw continuously

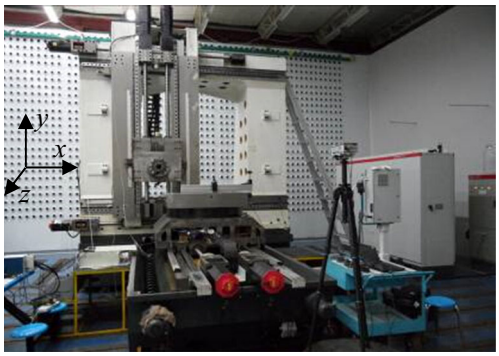

Fig. 1 CNC precision boring machine tool

during rotation. Meanwhile, a laser interferometer is used to measure the thermal error distribution at some specified time. When the ball screw is operating, the system keeps generating heat. After a certain time interval, the feed drive system stops to carry out measurement. The table moved step by step (the increment of each step is 100 mm) and the positioning errors are obtained at each step. Having finished data acquisition, the feed drive system starts to run again and goes on generating heat for measurement in the next cycle. There is a grating ruler located in parallel with screw shaft to detect the worktable position and assist to implement the closed loop motion control.

In this study, different feed rates (6, 12, 18 m/min) along the *x*-axis are considered. The worktable reciprocates along the *x*-axis with a stroke of 1000 mm. The thermal errors are measured every 40 min until the temperature reaches a steady state. Based on the mathematical analysis of the experimental results, we proposed a reduced error predicting method, and verifications under different conditions are performed.

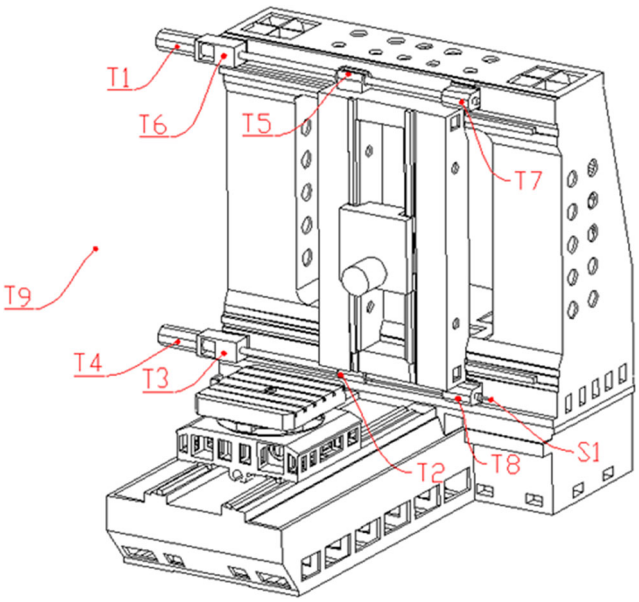

Fig. 2 Temperature points measured in the experiment

3 Thermal effect measurement and analysis

In order to analyze the thermal behavior of the precision boring machine tool, experiments are carried out with the machine tool running at two different feed speeds of 6 and 12 m/min. Results are compared as shown in Fig. 4. It can be seen that the temperature curves keep waving through except for ambient temperature, since the measurement of positioning error is performed at a lower speed of 2 m/min. Because the synchronization of ball screws is controlled in the master/salve way, the motor, bearing, and nut affiliated to the upper ball screw generate more heat than the lower one. Of all heat-generating components, the electric motor gives the largest temperature rise, and the nut comes second. During the experiment, the thermal equilibrium can be reached after running for over 500 min. After that, the temperature at every heat-generating point remains approximately constant. Higher feed speed contributes to a higher steady-state temperature. For instance, the upper motor temperature finally rises to about 30.5 °C at the speed of 6 m/min, but 38.1 °C at the speed of 12 m/min. Owing to the air conditioning devices enormously distributed on the lab wall as shown in Fig. 1, the ambient temperature maintains within 20±0.2 °C, minimizing its influence on heat generation and transfer process.

Generally, the effect of temperature change on a piece of metallic material is a small change in size and hence strain. As for the slender ball screw, study is usually focused on the thermal expansion in axial direction. As shown in Fig. 5, the axial length change is measured by sensor S1 located in Fig. 2. Because the thermal expansion is proportional to its temperature change approximately, the measurement results go up and down corresponding to temperature rise and fall. However, it appears that changes in ball screw length lag behind the pace at which temperature changes.

Temperature change of ball screw is the key factor leading to the thermal deformation. It is difficult to measure the surface temperature of the ball screw, so an infrared thermal camera is used to record the thermal image all the way. We select three typical points in axial direction with the coordinates of 150, 650, and 1050 mm. Figure 6 shows the surface temperature at these points that varies with position and time. Before heated, temperature difference between front and rear ends hardly exists. With continuous feeding, the temperature at one end becomes higher than the other. The temperature distributes linearly along the axis after achieving the steady state. From Fig. 6b, it can be seen that it takes less time for ball screw itself to reach thermal equilibrium compared with the other parts.

Thermal effect of ball screw feed drive system reflects from the thermally induced positioning error ultimately, as

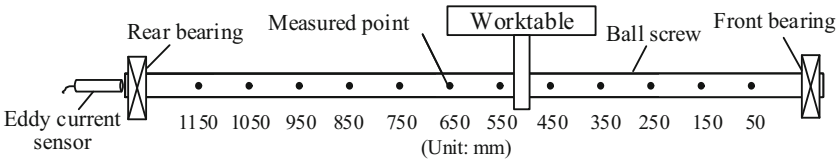

Fig. 3 Schematic of thermal error measurement in side view. No close-up shot for that location

shown in Fig. 7. Measured using a laser interferometer, the error increases with time in response to temperature change presented above. It proves that higher temperature rise results in larger thermal deformation thereby more positioning error. When the ball screw reaches thermal equilibrium, positioning errors at all measuring points also stop changing.

In addition, we can give the positioning error of the ball screw at a certain time, as shown in Fig. 8. It is quite similar to the temperature distribution along ball screw shaft increasing with the coordinate of measuring point. However, positioning error does not change much with the measuring point position at the starting time, because every point on the ball screw surface has the same temperature about equal to room temperature.

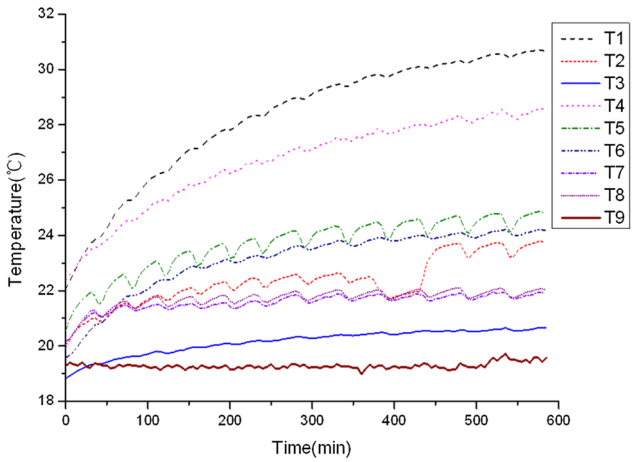

(a) Feeds speed is 6m/min

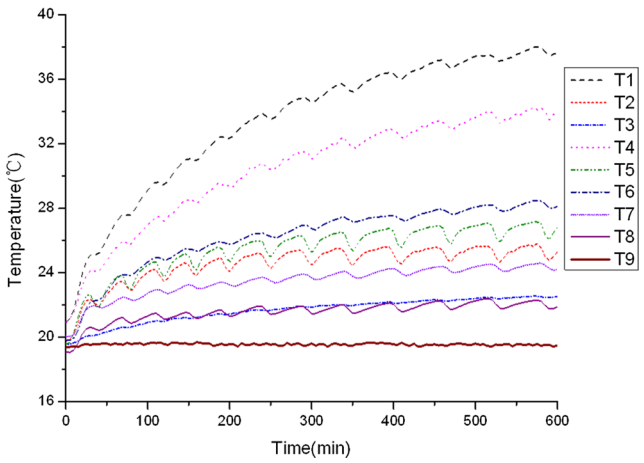

(b) Feed speed is 12m/min

Fig. 4 Temperature rise at different measuring points. **a** Feed speed is 6 m/min and **b** feed speed is 12 m/min

4 Modeling and prediction of thermal error

In order to reduce the thermally induced error, error compensation should be conducted while the machine tool is working. In fact, it is impractical to measure the positioning error when a cutting tool is machining a work piece at high rotating speed. So, it is the best choice to build an error prediction model to predict the time-dependent positioning error and compensate it through programing in computerized numerical controller.

4.1 Thermal expansion-based error prediction

(a) Temperature distribution of ball screw

Thermally induced positioning error and axial expansion of screw shaft occur in feed drive system simultaneously. Temperature rise directly causes elongation of the ball screw, consequently exerts an influence on positioning accuracy. Hence, in order to estimate the thermally induced positioning error effectively, temperature distribution of the ball screw should be investigated first.

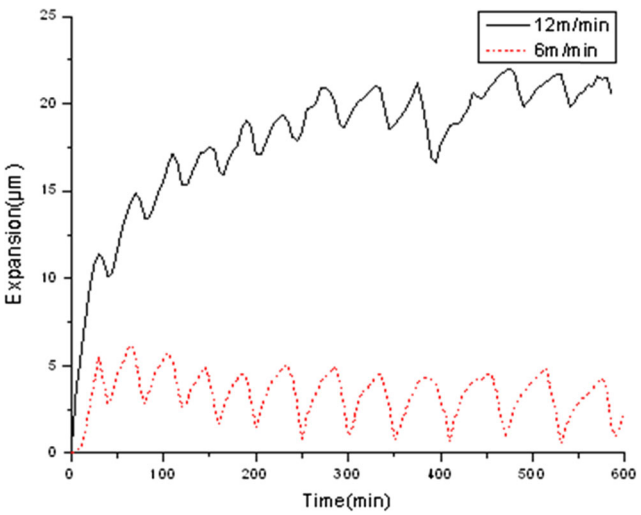

Fig. 5 Thermal expansion of ball screw at different speeds

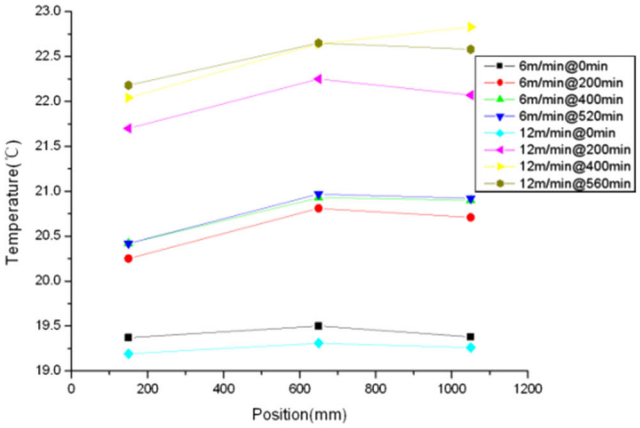

(a) Temperature vs position

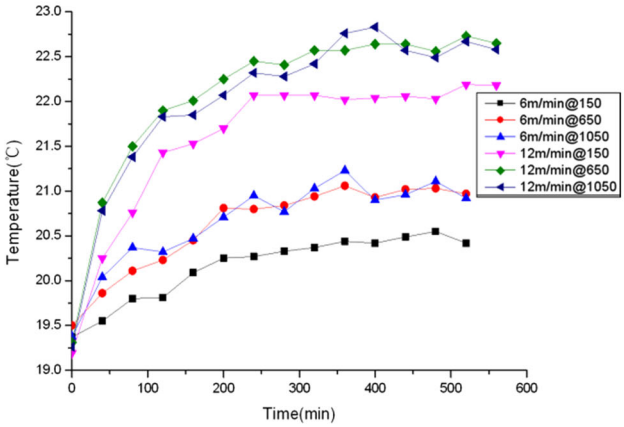

(b) Temperature vs time

Fig. 6 Temperature at different points of ball screw surface. **a** Temperature vs position and **b** temperature vs time

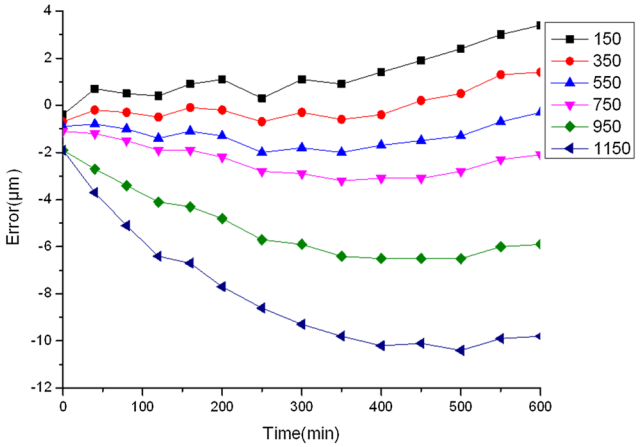

(a) Feed speed is 12m/min

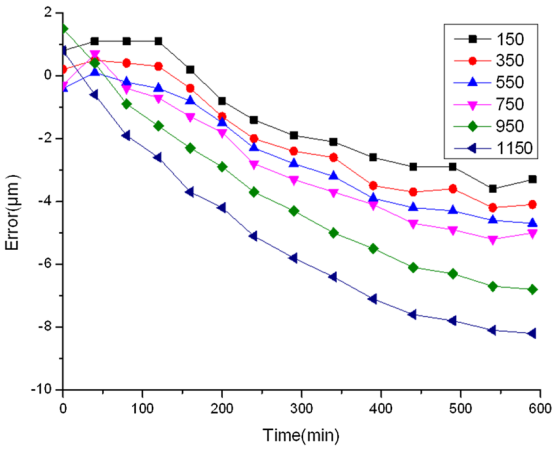

(b) Feed speed is 6m/min

Fig. 7 Thermally induced positioning error at different points. **a** Feed speed is 12 m/min and **b** feed speed is 6 m/min

In order to obtain the analytical solution of temperature distribution of ball screw, a one-dimensional model is dealt with equivalently to address the issue. Heat transfer equation is formulized as

$$\frac{\partial^2 T(x,t)}{\partial x^2} = \frac{\rho c}{\lambda}\frac{\partial T(x,t)}{\partial t} + \frac{4h}{\lambda d_0}\Delta T \tag{1}$$

where x is the coordinate on the ball screw axis, λ is the thermal conductivity, ρ is the density, c is the heat capacity, h is the convective heat transfer coefficient, d_0 is the nominal diameter, and ΔT is the temperature change. When achieving equilibrium state, the items on the right of the above equality are assumed to be zero. Since thermal equilibrium state is the main concern of this research, it can be deduced that temperature change is approximately linear with the x position on the ball screw in accordance with the results in Fig. 6a.

As for the temperature of a certain point on ball screw at any time, it can be expressed as

$$T(x_0,t) = k_T x_0 + b_T \tag{2}$$

where x_0 denotes the position of a certain point and k_T and b_T are coefficients can be easily obtained by linear interpolation.

On the other hand, the temperature change of a certain point at any time can be measured in the experiment, as shown in Fig. 9. Choosing three measuring points and fitting the data with exponential function, it yields a satisfactory result with the goodness of fitting R^2 larger than 0.98. So, we also have

$$T(x_0,t) = T_0 + c_T e^{-\tau t} \tag{3}$$

where T_0 is the reference temperature, c_T is the coefficient, and τ is a time constant. Combining the

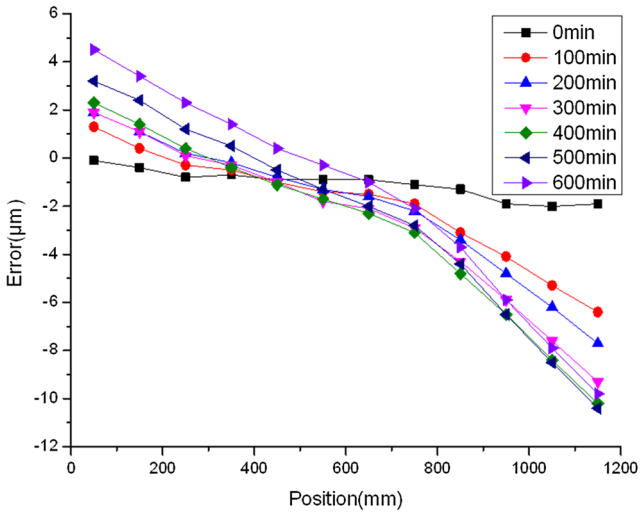

(a) Feed speed is 12m/min

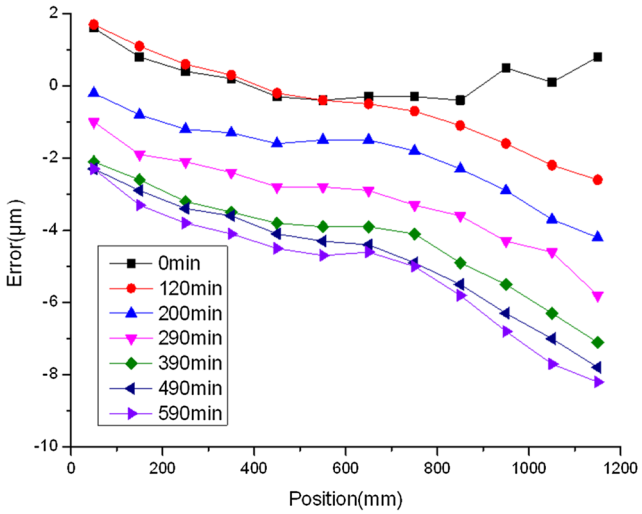

(b) Feed speed is 6m/min

Fig. 8 Thermally induced positioning error at different times. **a** Feed speed is 12 m/min and **b** feed speed is 6 m/min

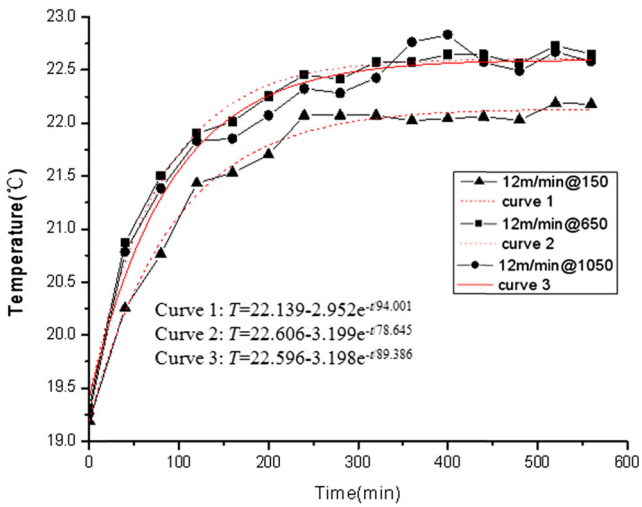

Fig. 9 Temperature change in different positions at 12 m/min

above equations, the temperature expression can be changed into

$$T(x,t) = \frac{k_T x + b_T}{k_T x_0 + b_T}(T_0 + c_T e^{-\tau t}) \tag{4}$$

In order to get the result of Eq. 4, we must select a point as a reference position. Another parameter to be determined is T_0; it can be taken as the initial temperature of the ball screw with a small error tolerance according to experimental verification.

(b) Thermal expansion

If there is a bar element and its temperature distribution is described as Eq. 4, then the total thermal expansion of the bar is

$$\Delta L = \int_0^L \alpha \Delta T(x,t)dx = \int_0^L \alpha(T(x,t) - T_0)dx \tag{5}$$

where ΔL is the thermal expansion, L is the original length of the bar, ΔT is the temperature rise, and α is the thermal expansion coefficient. It is indicated in Fig. 10 that the thermal expansion in length is proportional to the enclosed area under the temperature distribution curve.

In the experiment, the thermal expansion of ball screw can be measured online with an eddy current displacement sensor. The measured data reflects the thermal expansion accumulation at the free end because the ball screw is usually simply supported. For a solid ball screw without cooling fluid inside, it is easy to perform in situ measurement.

(c) Relationship between thermal error and expansion

Unlike the thermal expansion of the ball screw which can be obtained regardless of whether it operates or not, thermally induced error measuring and normal ball screw feeding have to clash. So, it is necessary to predict the thermal error of the ball screw real timely with the help of thermal expansion online measurement, and the relationship between them needs to be investigated.

According to experimental results, the thermally induced positioning error of the ball screw varies

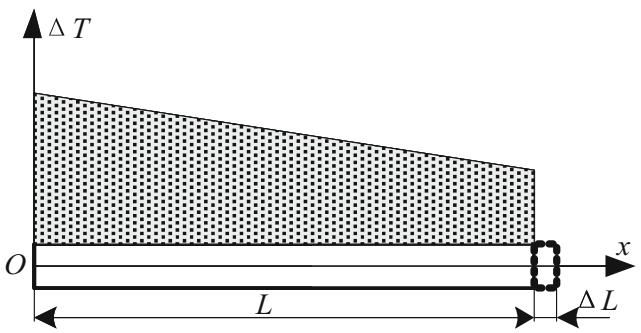

Fig. 10 Thermal expansion of a bar

with different worktable position. It is quite similar to the temperature distribution along the ball screw because the error is caused by a temperature rise in essence. Take the experimental results obtained at the speed of 12 m/min into consideration, data also can be fitted with linear interpolation, as shown in Fig. 11a. We choose the results at three different times including start time, and they are all in agreement with the fitting line. So, the thermal error of the ball screw system at some time can be written as

$$E(x, t_0) = k_E x + b_E \tag{6}$$

where k_E and b_E are coefficients can be obtained by linear interpolation.

In response to the temperature change, the thermal error of the ball screw system varies with time nonlinearly. Fitted with a polynomial of degree 3, we can find the approximate expressions to reveal the relationship between thermal error and time at a given position, as shown in Fig. 11b. This nonlinear relationship can be written as

$$E(x_0, t) = A_E t^3 + B_E t^2 + C_E t + D_E \tag{7}$$

where A_E, B_E, C_E, and D_E are coefficients to be determined.

In consideration of time-variant temperature, the thermal error can be estimated by the following equation:

$$E(x_a, t_a) = (k_E x_a + b_E)\left(A_E {t_a}^3 + B_E {t_a}^2 + C_E t_a + D_E\right) \tag{8}$$

where x_a and t_a are any position and any time corresponding to the temperature set. It should be noticed that all coefficients in the above equality is not constant. For instance, k_E and b_E are varying with time while the rest with position. Likewise, we derive this equation on the basis of linear distribution of thermal error along ball screw shaft. Therefore, the reference point should be properly chosen for predicting calculation.

In fact, the thermal error has a close relation with both time and position when the ball screw system is operating. So, the thermal error data collected in the experiment will make up an $m \times n$ matrix, where m and n are the number of measuring point and time interval, respectively. Apparently, the bigger the values of m and n are, the more accurate the predicting results become. So, in order to predict the thermal error correctly, we should firstly obtain the following matrix.

$$E_{m\times n} = E_x E_t = [e_{1t} \cdots e_{mt}] \begin{bmatrix} e_{x1} \\ \vdots \\ e_{xn} \end{bmatrix} \tag{9}$$

where e_{it} (i=1…m) and e_{xj} (j=1…n) are position-dependent and time-dependent error components, respectively.

Combining with Eq. 5, we can calculate the thermal error of the ball screw system given that the axial thermal expansion is real timely measured. Actually, we develop the relationship between them with temperature acting as an intermediate variable because the temperature of ball screw located under the moving worktable is difficult to measure.

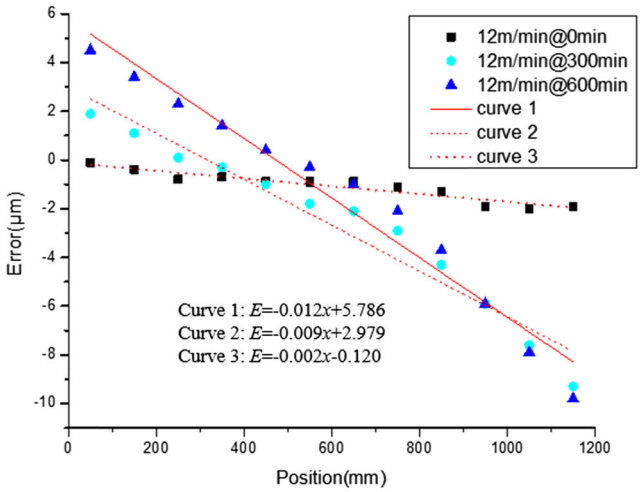

(a) Errror vs position

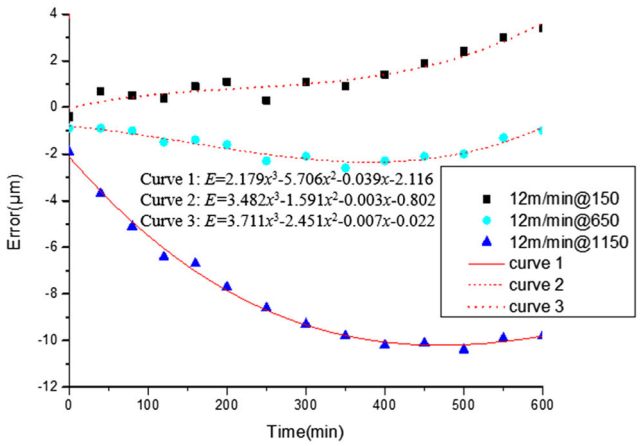

(b) Error vs time

Fig. 11 Data fitting results of thermal error at 12 m/min. **a** Error vs position and **b** error vs time

4.2 Error prediction modeling based on temperature point optimization

In order to reduce the thermal effect on machining accuracy, cooling systems are sometimes installed on the machine tool to pursue a strict regulation of temperature rise. In those cases, cooling pipes are fixed on the end surface of the ball screw. As shown in Fig. 12, it is very difficult to measure the axial

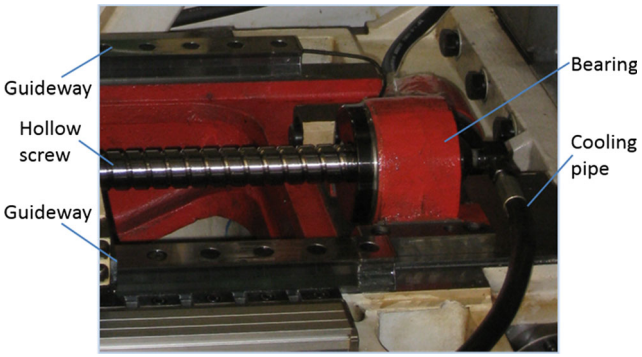

Fig. 12 A ball screw drive with circulation oil cooling

expansion of the ball screw in the same way as illustrated in the above section. Under this circumstance, we need to explore an alternative by establishing the relationship between the temperatures of the selected critical points and the thermal error of the ball screw.

(a) Temperature measurement optimization

Although we can place as many thermocouples as possible at different locations of the machine tool to obtain lots of temperature data, error modeling with enormous temperatures acting as the variables of the thermal error function is too complicated to put into application. It is preferred that we should extract the temperature data contributing to the thermal error most. According to statistics and the related knowledge of data analysis, fuzzy clustering is a very effective way to divide data elements into classes or clusters so that items in the same class are as similar as possible, and items in different classes are as dissimilar as possible [23]. It has found many applications in variety of fields, showing good characteristics in data classification as clustering the temperature data for thermal issues. Generally, clustering of given sample data follows the steps sketched in Fig. 13.

The sample data obtained in the experiment are composed of a temperature matrix T_{ij}, $i=1\ldots9$, corresponding to the nine temperature sensors deployed on the ball screw system; $j=1\ldots N$ is the number of the data collected from one sensor. Detailed clustering procedures and rules are not concerned as it can be conducted with running the functions in MATLAB. However, we should choose proper algorithm for each data processing step [24].

After dividing the sample data into classes, we gather the variables with a similar attribute together. Now, we have to select the critical variables from each group and decide the temperature to which the thermal error is sensitive most. So, a correlation coefficient $\rho_{T,E}$ is defined as follows to determine the temperature that has closest relations with the thermal error.

$$\rho_{T,E}=\frac{\sum_{j=1}^{n}\left(T_{ij}-\overline{T}_i\right)\left(E_j-\overline{E}_j\right)}{\sqrt{\sum_{j=1}^{n}\left(T_{ij}-\overline{T}_i\right)^2}\sqrt{\sum_{j=1}^{n}\left(E_j-\overline{E}_j\right)^2}} \tag{10}$$

where T_{ij} is the component of T_{ij}, E_j is the thermal error, $\overline{T}_i$ is the mean value of the temperature, and $\bar{E}_j$ is the mean value of the thermal error.

Referring to the correlation coefficients of different temperature combinations, the critical temperature variables can be determined. Because the feed drive is a dual ball screw system, we actually take the lower one into account for simplicity. The temperature variable whose coefficient is higher in each cluster is selected as a critical variable. Finally, we choose T_3, T_8, and T_9 as the critical temperature variables. It is noticed that the temperature of nut and servo motor is not selected. This can be explained by the heat transfer process illustrated in Fig. 14. It describes the general heat exchange between the ball screw, heat sources, and surroundings. Thermal radiation is not considered in this process because the component temperature cannot reach that high level usually. The heat transfer of ball screw system mainly consists of heat conduction from nut Q_N, from bearings Q_S, and electric motor Q_M, as well as heat loss Q_S to the surrounding air by natural convection. It is shown in the results that Q_N will counterbalance Q_S approximately and Q_M also can be neglected by incorporating its contribution into an equivalent Q_B. Consequently, heat transfer for ball screw will be changed into a one-dimensional issue. The heat generated at double ends of the ball screw conducts in the axial direction and contributions add up at the corresponding position. The results coincide with the results presented in the previous sections.

With those optimized temperature variables, the thermally induced error can be modeled and predicted easily. Generally, we can express the problem as solving the following matrix equation

$$T_{ij}{}^{T}R=E_j \tag{11}$$

where $E_j=[E_1\ldots E_N]^T$ is the thermal error matrix made up of measured data and R is the matrix with the same

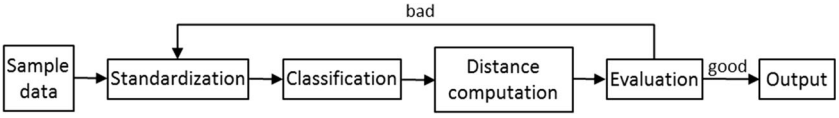

Fig. 13 Flow chart of fuzzy clustering method

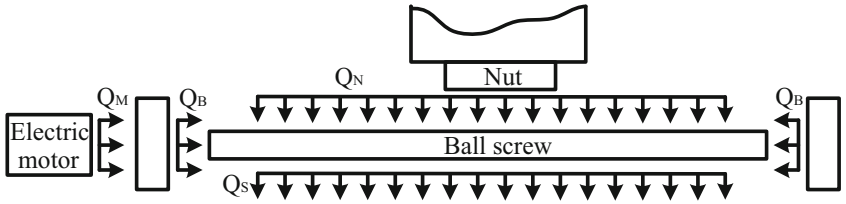

Fig. 14 Schematic of heat transfer of ball screw drive system

dimensions as E_j and required to be determined. It is noticed that R should include at least one nonzero element.

(b) Thermal error modeling

Now that there exist critical temperature points having the closest relations with thermally induced error, models to describe this relations mathematically should be created. In light of multiple temperature variables, multiple linear regression method widely employed in statistical analysis of situations that cannot be explained by a deterministic model explicitly will be a best solution. Also, it has already been applied in analyzing the thermal error of machine tools by other researchers previously [25]. Modeling is based on the assumption that the dependent and independent variables are linearly associated with each other; hence, the relationship can be written as [26]

$$y = b_0 + b_1x_1 + b_2x_2 + \cdots + b_mx_m + \varepsilon \quad (12)$$

where y is the dependent variable of thermal error, x_i (i= 1…m) are independent variables of temperature, $b_0 \ldots b_m$ are coefficients to be determined, and ε is a residual. Here, m is the number of critical temperature, and m= 3. With measured temperature data, we can compute the unknown parameters in the model through least squares estimation method. This work can be done in MATLAB with regress functions.

Figures 15 and 16 show the predicted results with multiple linear regression models at the speed of 6 and 12 m/min, respectively. Comparisons between measured and predicted data are presented. We consider the thermal error changes with time at two different coordinates of 50 and 1150 mm in the x-axis. The regression equations are obtained as follows

$$\begin{aligned}
&6\ \text{m/min, at 50 mm}: \\
&\quad y = 56.092 + 0.267x_1 - 6.594x_2 + 3.198x_3 \\
&6\ \text{m/min, at 1150 mm}: \\
&\quad y = 61.832 - 0.786x_1 - 3.981x_2 + 1.581x_3 \\
&12\ \text{m/min, at 50 mm}: \\
&\quad y = -139.215 + 0.138x_1 + 8.866x_2 - 1.762x_3 \\
&12\ \text{m/min, at 1150 mm}: \\
&\quad y = -41.021 - 0.841x_1 - 1.698x_2 + 4.654x_3
\end{aligned}$$

From Figs. 15a and 16a, we can see that the regression models can predict the thermal error with a relatively high goodness of fitting throughout the entire heat-generating process, except for some data in the first hour. Comparing the results under two different speeds, it can be seen that the measured and predicted data get closer with time and higher predicting accuracy can be reached when the worktable is moving to the far end of the ball screw. Moreover, it seems as if the prediction models have less stability to predict the errors of small displacement points..

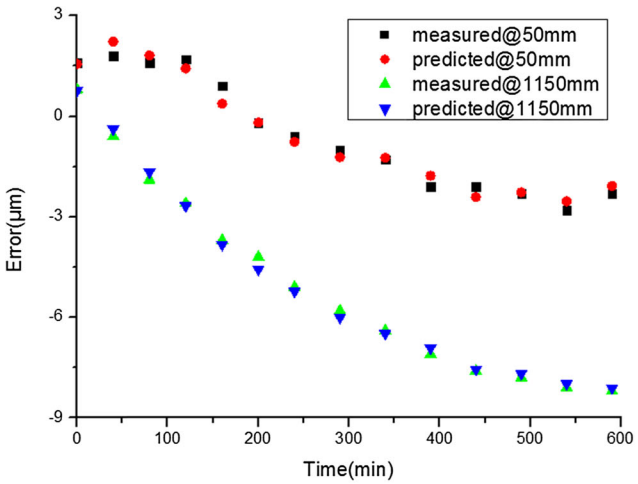

(a) Error prediction results

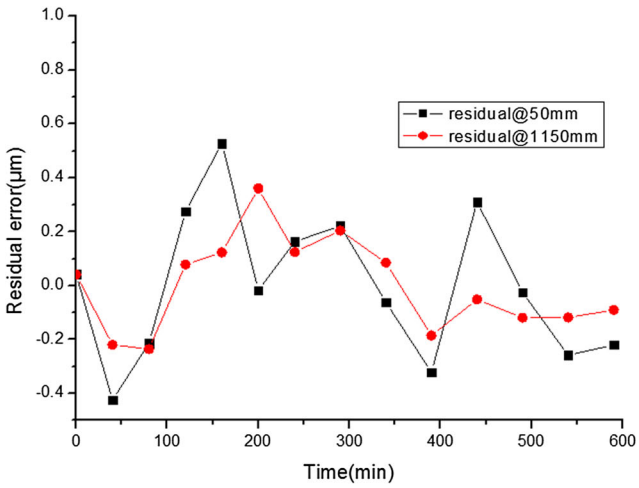

(b) Residual error

Fig. 15 Thermal error prediction result of 6 m/min feed speed. **a** Error prediction results and **b** residual error

In order to explain the predicted results more clearly, residual errors produced in modeling and predicting processes are also plotted as shown in Figs. 15b and 16b. Residuals in prediction with 6 m/min feed speed is much smaller than those with 12 m/min, having a maximum approximately limited within ±0.5 μm. This also has relations with the fact that lower speed working conditions generate less heat thereby smaller thermally induced errors than high-speed case. After all, a great majority of data turn out to be falling into the expected residual section.

It is assumed that the thermal error distributes linearly in the axial direction at a certain time. So, the coefficients in Eq. 12 should not be constant but incorporating a linear polynomial with the variable x. For example, $b_m=k_{xm}x+b_{xm}$, where k_{xm} and b_{xm} are position variants. Their values can be calculated by means of least squares estimate on the basis of the regression equations of different positions.

5 Experimental validations

In order to verify the proposed thermal error predicting methods, experiments are carried out on the precision machine tool presented in Section 2. The error prediction procedure is sketched in Fig. 17, including data acquisition, model establishment, and verification. For each working condition to be considered, a great number of data from experimental measurement are required for modeling and predicting, so a suite of software and hardware should be developed at the ready for measurement. Error modeling of different conditions is done in the same way as before. It is really difficult to collect and process so much data because more than 10 h may be taken to get a group of desired data. Moreover, two points should be noted as follows.

1. Reference points have to be raised when modeling the relationship between thermal error and position on the ball screw. With the reference point, linear distribution of thermally induced error along screw shaft can be expressed mathematically no matter duration and speed varies.
2. According to Eq. 5, thermal expansion in length is a quadratic function for the independent variable x. This is deduced on assumption that heat transfer through ball screw is taken as a one-dimensional heat conduction problem in the axial direction approximately. As determined by linear fitting results, the thermal error calculation model expressed in Eq. 8 is a linear function of displacement x. So, the relationship between $E(x)$ and ΔL is built with a linear polynomial in x demonstrating that elongation effect is accumulated linearly in the axial direction.

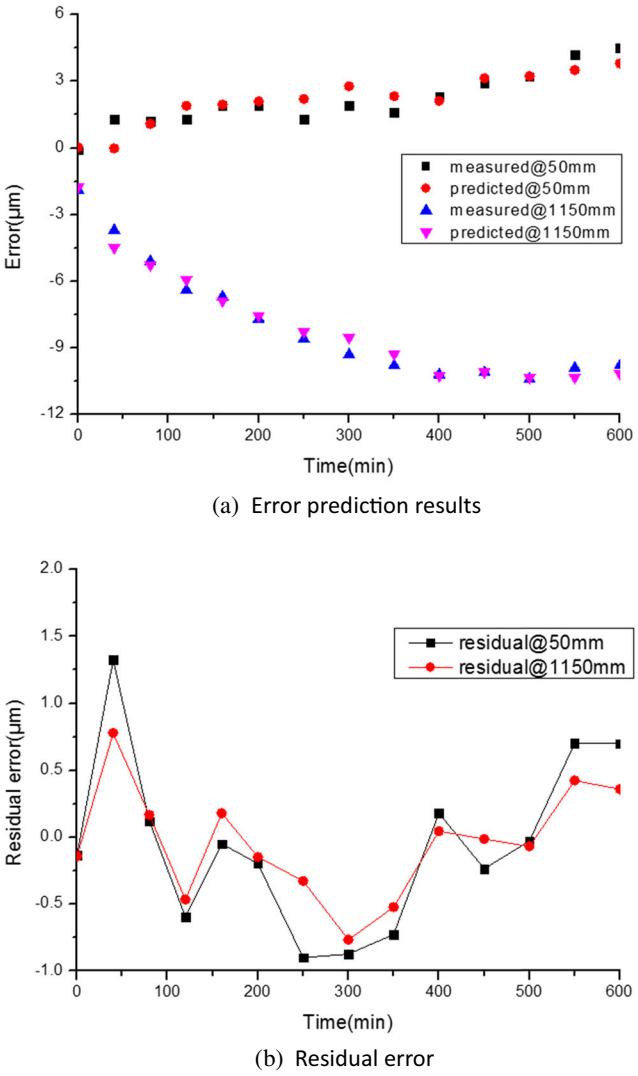

Fig. 16 Thermal error prediction result of 12 m/min feed speed. **a** Error prediction results and **b** residual error

Before investigating into the thermally induced error distribution and variation, we measure the axial elongation of the dual ball screw system under continuous heating conditions as shown in Fig. 18. In contrast with the previous results, the temperature in this measurement keeps rising all the time until achieving steady state. So, it takes a relatively shorter period of time. The results also indicate that synchronization is a very important issue in such dual drive system. Two ball screws make a difference of more than 10 μm in thermal expansion,

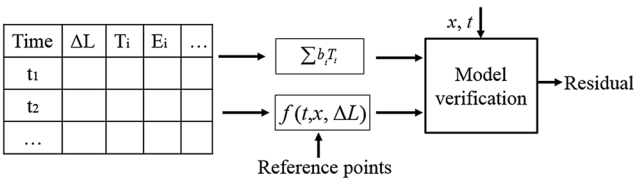

Fig. 17 Schematic diagram of thermal error prediction procedure

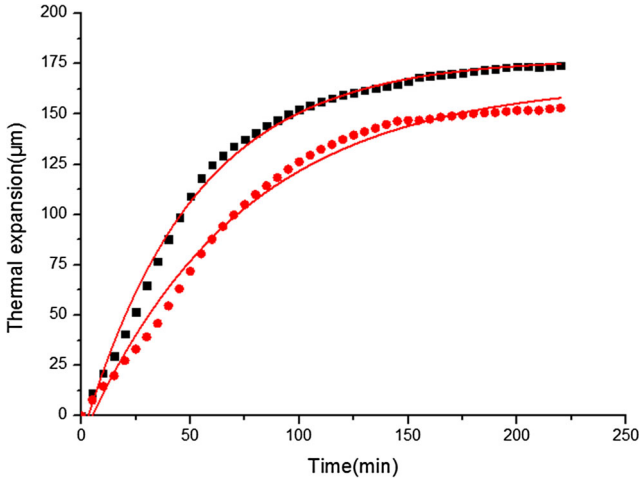

Fig. 18 Thermal expansion of ball screws by continuous running. *Dots* represent the measured data while *lines* are trend lines drawn according to the calculation results based on Eq. 5

exerting an influence on motion synchronization. In practice, this difference is also coordinated by the moving mechanical parts and behaves as an equivalent error eventually. In Fig. 18, dots represent the measured data while lines are trend lines drawn according to the calculation results based on Eq. 5.

Experimental verifications are conducted with the feed drive system operating at the speed of 18 m/min. Figure 19 shows the results obtained by method I of thermal expansion-based prediction. In order to use the statistic modeling results under two working conditions of 6 and 12 m/min, a weight is introduced into the mathematical expressions. Coefficients in Eq. 8 are weighted and accumulated, respectively, corresponding to two kinds of speed given beforehand. In addition, this work is also completed partly in the presence of the theoretical models of the working condition to be predicted. Firstly, expressions as Eqs. 6, 7, and 8 for each working condition are obtained. Then, coefficients ahead of the corresponding items are picked out to establish the weighted relations. Finally, modifications of coefficients in the predicted models are made on the basis of previously fitted results. It can be seen in Fig. 19a that the predicted results and the measured data marked with dots are in good agreement with each other. The residual error shown in Fig. 19b distributes normally with the highest value falling in the range of ±2 μm. Moreover, it turns out to be even smaller at the positions far away from the origin.

Figure 20 shows the results obtained by method II of critical temperature-based perdition. It involves

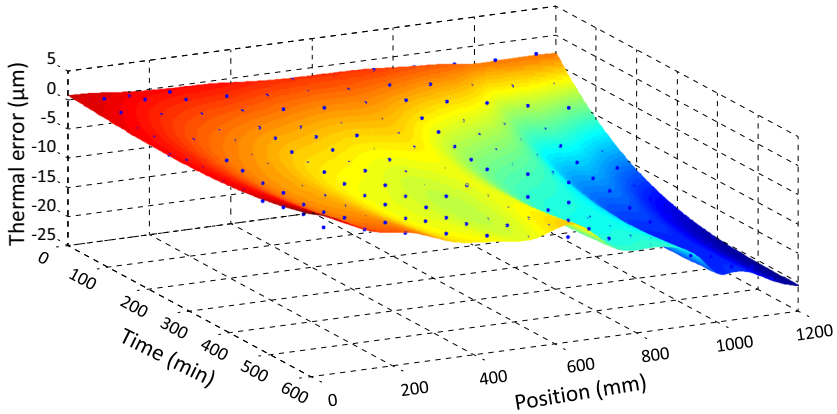

(a) Thermal error (measured data marked with dots)

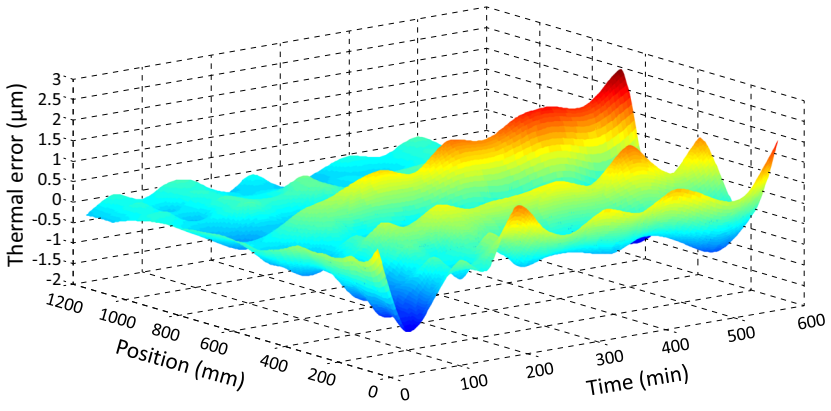

(b) Residual distribution

Fig. 19 Thermal prediction results by method I. **a** Thermal error (measured data marked with *dots*) and **b** residual distribution

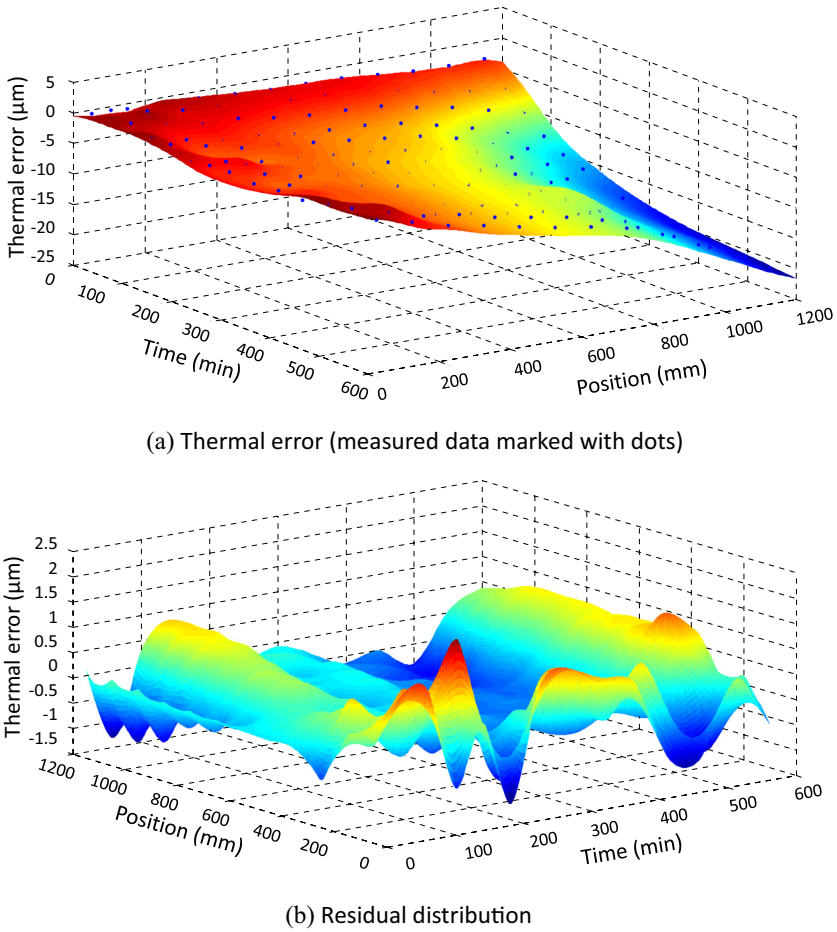

Fig. 20 Thermal prediction results by method II. **a** Thermal error (measured data marked with *dots*) and **b** residual distribution

establishing the relationships between thermal error and critical temperatures by multiple linear regression analysis as well as exploring the thermal error variation with different measuring position by least squares estimation. In contrast to method I, temperature data are dealt with here. Coefficients in the regression model are firstly obtained as a constant and then formulated into a position-dependent expression, because time is included when considering temperature change. The curved surface of the thermal error shown in Fig. 20a is quite similar to that in Fig. 19a. The residual error shown in Fig. 20b is smaller than that in Fig. 19a with the maximum about 1.5 μm. The colored map reveals the relationship between thermal error and time and position, consecutively, in contrast with the scattered points obtained by measurement. The different colors in Fig. 20 are demonstrating the contour map of errors and residuals at the different levels. It is shown in the results that the predicting accuracy is high enough to replace the measurement and reflect the thermal characteristics of feed drive system in terms of induced error. It should be noticed that the prediction accuracy appears relatively higher in the latter period during operation, coinciding with the assumption that one-dimensional heat transfer in the axial direction remains after the feed drive system achieves thermal equilibrium.

6 Conclusions

This paper explores the relationships between the thermal error of feed drive system and the axial thermal expansion as well as temperature of ball screw. It works out the method for thermal error modeling and calculation easy to perform in actual application with the least number of the most critical measured variables. Based on the research work, some conclusions can be drawn as follows.

(1) Thermal error is a key influential factor of machining accuracy, varying with feed speed, working time, and travel distance of feed drive system. As for a dual ball screw feed drive system, the thermally induced non-synchronization is inevitable as a result of the different thermal behavior of ball screws.
(2) Thermal expansion of ball screw in the axial direction causes thermal drift and has direct relation with thermally induced error. The thermal error change along the axis is approximately linear while the variation with working time is nonlinear. By real timely detecting the thermal expansion of the ball screw, we can model and predict the thermal error distribution in both time and position domain.

(3) It proves that there exist critical heating points with which we can obtain the heat conduction result equivalently. And the thermal issue of the ball screw can be taken as a one-dimensional heat transfer model when the feed drive system reaches a thermal equilibrium state. By collecting the temperature data at the critical points, thermal error can be made with mathematical modeling properly.

Acknowledgments This study was supported by the Innovative Research Group Fund of National Natural Science Foundation of China (No. 51221004), Open Fund of State Key Laboratory of Fluid Power Transmission and Control at Zhejiang University (No. GZKF-201409), and Special Financial Grant from the China Postdoctoral Science Foundation (No. 2014T70910).

References

1. Josef M, Jerzy J, Eckart U, Malkan D, Wolfgang K (2012) Thermal issues in machine tools. CIRP Ann Manuf Technol 61:771–791
2. Yang J, Shi H, Feng B, Zhao L, Ma C, Mei XS (2015) Thermal error modeling and compensation for a high-speed motorized spindle. Int J Adv Manuf Technol 77:1005–1017
3. Uriarte L, Herrero A, Zatarain M, Santiso G, Lacalle LN, Lamikiz A, Albizurib J (2007) Error budget and stiffness chain assessment in a micromilling machine equipped with tools less than 0.3 mm in diameter. Precis Eng 31:1–12
4. Díaz-Tena E, Ugalde U, Lacalle LN, Iglesia A, Calleja A, Campa FJ (2013) Propagation of assembly errors in multitasking machines by the homogenous matrix method. Int J Adv Manuf Technol 68:149–164
5. Arizmendi M, Fernandez J, Lacalle LN, Lamikiz A, Gil A, Sánchez JA, Campa FJ, Veiga F (2008) Model development for the prediction of surface topography generated by ball-end mills taking into account the tool parallel axis offset. Experimental validation. CIRP Ann Manuf Technol 57:101–104
6. Wang HT, Wang LP, Li TM, Han J (2013) Thermal sensor selection for the thermal error modeling of machine tool based on the fuzzy clustering method. Int J Adv Manuf Technol 69:121–126
7. Liang YC, Su H, Lu LH, Chen WQ, Sun YZ, Zhang P (2015) Thermal optimization of an ultra-precision machine tool by the thermal displacement decomposition and counteraction method. Int J Adv Manuf Technol 76:635–645
8. Kim SK, Cho DW (1997) Real-time estimation of temperature distribution in a ball screw system. Int J Mach Tools Manuf 37:451–464
9. Ming X, Jiang X (2011) A thermal model of a ball screw feed drive system for a machine tool. Proc Inst Mech Eng C J Mech Eng Sci 225:186–193
10. Ahn JY, Chung SC (2004) Real-time estimation of the temperature distribution and expansion of a ball screw system using an observer. Proc Inst Mech Eng B J Eng Manuf 218:1667–1680
11. Otakar H (2007) Thermo-mechanical model of ball screw with non-steady heat sources. Int Conf Therm Issues Emerg Technol Theory Appl 1:133–137
12. Wu CH, Kung YT (2003) Thermal analysis for the feed drive system of a CNC machine center. Int J Mach Tools Manuf 43:1521–1528
13. Huang SC (1995) Analysis of a model to forecast thermal deformation of ball screw feed drive systems. Int J Mach Tools Manuf 35:1099–1104
14. Yun WS, Kim SK, Cho DW (1999) Thermal error analysis for a CNC lathe feed drive system. Int J Mach Tools Manuf 39:1087–1101
15. Wu CW, Tang CH, Chang CF, Shiao YC (2012) Thermal error compensation method for machine center. Int J Adv Manuf Technol 59:681–689
16. Wang W, Zhang Y, Yang J, Zhang YS, Yuan F (2013) Geometric and thermal error compensation for CNC milling machines based on Newton interpolation method. Proc Inst Mech Eng C J Mech Eng Sci 227:771–778
17. Hsieh MF, Chang WC (2012) Combining full and semi closed loop synchronous control for dual mechanically coupled ball screw system. Int J Comput Appl Technol 45:139–147
18. Mayr J, Ess M, Weikert S, Wegener K (2010) Comparing different cooling concepts for ball screw systems. Proceedings of ASPE Annual Meeting
19. Xu ZZ, Liu XJ, Lee IB, Ahn IS, Lyu SK (2013) A study on heat generation control of a precision ball screw drive system. Adv Mater Res 68:360–363
20. Xu ZZ, Liu XJ, Kim HK, Shin JH, Lyu SK (2011) Thermal error forecast and performance evaluation for an air-cooling ball screw system. Int J Mach Tools Manuf 51:605–611
21. Yang AS, Cai SZ, Hsieh SZ, Kuo TC, Wang CC, Wu WT, Hsieh WZ, Hwang YC (2013) Thermal deformation estimation for a hollow ball screw feed drive system. Proceedings of the World Congress on Engineering, Vol. III
22. Liu YP, Chen Z, Rui ZY (2013) Design and simulation of gas-liquid binary cooling system for high-speed ball screw units. Chin Mech Eng 24:95–98
23. Frank H (1999) Fuzzy cluster analysis: methods for classification, data analysis and image recognition. John Wiley & Sons
24. Yang J, Shi H, Feng B, Zhao L, Ma C, Mei XS (2014) Applying neural network based on fuzzy cluster pre-processing to thermal error modeling for coordinate boring machine. Procedia CIRP 17:698–703
25. Ramesh R, Mannan MA, Poo AN (2000) Error compensation in machine tools-a review: part II: thermal errors. Int J Mach Tools Manuf 40(9):1257–1284
26. Montgomery DC, Peck EA, Vining GG (2006) Introduction to linear regression analysis. John Wiley